

Research Report

Manipulation of the charge state of single Au atoms on insulating multilayer films

W. Steurer,¹ J. Repp,² L. Gross,¹ I. Scivetti,³ M. Persson,³ and G. Meyer¹

¹IBM Research-Zurich, 8803 Rüschlikon, Switzerland

²Institute of Experimental and Applied Physics, University of Regensburg, 93053 Regensburg, Germany

³Surface Science Research Centre and Department of Chemistry, University of Liverpool, Liverpool L69 3BX, United Kingdom

The final version of this paper appeared in *Phys. Rev. Lett.* **114**, 036801 (22 January 2015) and may be downloaded at <http://dx.doi.org/10.1103/PhysRevLett.114.036801>
© 2015 American Physical Society

LIMITED DISTRIBUTION NOTICE

This report has been submitted for publication outside of IBM and will probably be copyrighted if accepted for publication. It has been issued as a Research Report for early dissemination of its contents. In view of the transfer of copyright to the outside publisher, its distribution outside of IBM prior to publication should be limited to peer communications and specific requests. After outside publication, requests should be filled only by reprints or legally obtained copies (e.g., payment of royalties). Some reports are available at <http://domino.watson.ibm.com/library/Cyberdig.nsf/home>.



Research

Almaden – Austin – Beijing – Brazil – Cambridge – Dublin – Haifa – India – Kenya – Melbourne – T.J. Watson – Tokyo – Zurich

Manipulation of the charge state of single Au atoms on insulating multilayer films

W. Steurer,^{1,*} J. Repp,² L. Gross,¹ I. Scivetti,³ M. Persson,³ and G. Meyer¹

¹*IBM Research-Zurich, 8803 Rüschlikon, Switzerland*

²*Institute of Experimental and Applied Physics, University of Regensburg, 93053 Regensburg, Germany*

³*Surface Science Research Centre and Department of Chemistry,
University of Liverpool, Liverpool L69 3BX, United Kingdom*

(Dated: September 12, 2014)

We show charge-state manipulation of single Au adatoms on 2–11 monolayer (ML) thick NaCl films on Cu surfaces by attaching/detaching single electrons via the tip of an atomic force microscope (AFM). Tristate charge control (neutral, negatively charged, and positively charged) is achieved. On Cu(100) and Cu(111) supports, charge tristability is achieved independently of the NaCl layer thickness. In contrast, on Cu(311), only Au anions are stable on the thinnest NaCl films, but neutral and positive charge states become sufficiently long-lived on films thicker than 4 ML to allow AFM-based charge-state-manipulation experiments.

Stabilizing charge states of atoms and molecules, as well as controlled charge-state manipulation, is of great interest in the framework of molecular electronics and a prerequisite for single-electron-transport experiments on insulating films. It might seem natural to employ bulk insulators and bulk-like insulating films [1, 2] for these purposes, on which charge states are intrinsically stabilized by the suppression of charge transfer with the substrate. However, controlled manipulation of the charge state of single atoms and molecules is hampered by technical issues on these substrates and has to be shown yet. Perhaps the most severe difficulty is that scanning tunneling microscopy (STM) is ruled out by the insulating nature of the samples. So far, charge-state manipulation has only been shown for single atoms and molecules on bi- and trilayer NaCl films [3–6], on which STM operation is enabled by the still high tunneling probability through the film and charge states are stabilized by large ionic relaxations of the NaCl film. In contrast to charge stabilization on bulk insulators, the charge-state-stabilization mechanism on films with *non*-vanishing tunneling probability depends strongly on the specific properties of adsorbate, film, and substrate [4] and only selected charge states can be stabilized. Despite its important implications also for catalysis, the transition from films with non-vanishing tunneling probability to bulk-like insulating films [7–9] in the context of charge-state manipulation is poorly understood.

Here, we present a detailed study of Au adatoms adsorbed on 2–11 ML thick NaCl films, denoted as NaCl(2–11 ML), grown on Cu(100), Cu(111) and Cu(311). For the thickest films, we extend the charge-state control into regions where charges are stabilized by suppressing charge transfer with the substrate. In this film-thickness regime, charge-state control is achieved by attaching/detaching single electrons via the tip of an atomic force microscope (AFM). Owing to the single-electron sensitivity of the AFM, the passage of the electron from the tip to the Au atom (and vice versa) is observed as a jump in the frequency shift, Δf , and the

direction of the electron path is retrieved from the shift of the local contact potential difference (LCPD). We show that Au adatoms on NaCl exhibit charge tristability (neutral, negatively charged, and positively charged) irrespective of the film thickness on all Cu substrates except Cu(311). On Cu(311), which has a lower work function, only Au anions are stable on few ML thick films because of phonon-mediated electron transfer from the Cu(311) substrate through the NaCl film. However, the lifetime of the metastable neutral and positive states increases by two orders of magnitude per NaCl layer due to a reduction of the tunneling probability through the film. On NaCl(5 ML)/Cu(311), their lifetime is of the order of an hour, long enough to permit AFM-based charge-state-manipulation experiments.

The experiments described here were performed in a custom-built ultra-high vacuum (UHV) apparatus equipped with means for sample cleaning, thin-film preparation, and a combined low-temperature (LT) STM/AFM based on a qPlus tuning-fork sensor design [10]. The base pressure of the apparatus was lower than 1×10^{-10} mbar. NaCl films with thicknesses from 2–11 ML were prepared on Cu(111), Cu(100), and Cu(311) single crystal substrates following the procedure described in Ref. 11 and the Supplementary Material (SM) [15]. Au atoms were deposited onto the sample at 5 K by sublimation in vacuum.

The NaCl films on the different Cu substrates were characterized from topographical STM images, which were typically recorded at large applied sample biases, V , ($V > 4$ V) and small currents (< 1 pA). Well-ordered films with monoatomic steps between individual NaCl terraces were observed on all substrates; a typical STM image before Au deposition, which was recorded on a NaCl(6–11 ML)/Cu(111) film, is shown in Fig. SM1. The local film thickness was determined by a fingerprinting technique based on measuring the lifetime of the vacancy state of intentionally created chlorine vacancies by the tunneling current [11].

Figure 1 shows the manipulation of the charge state of

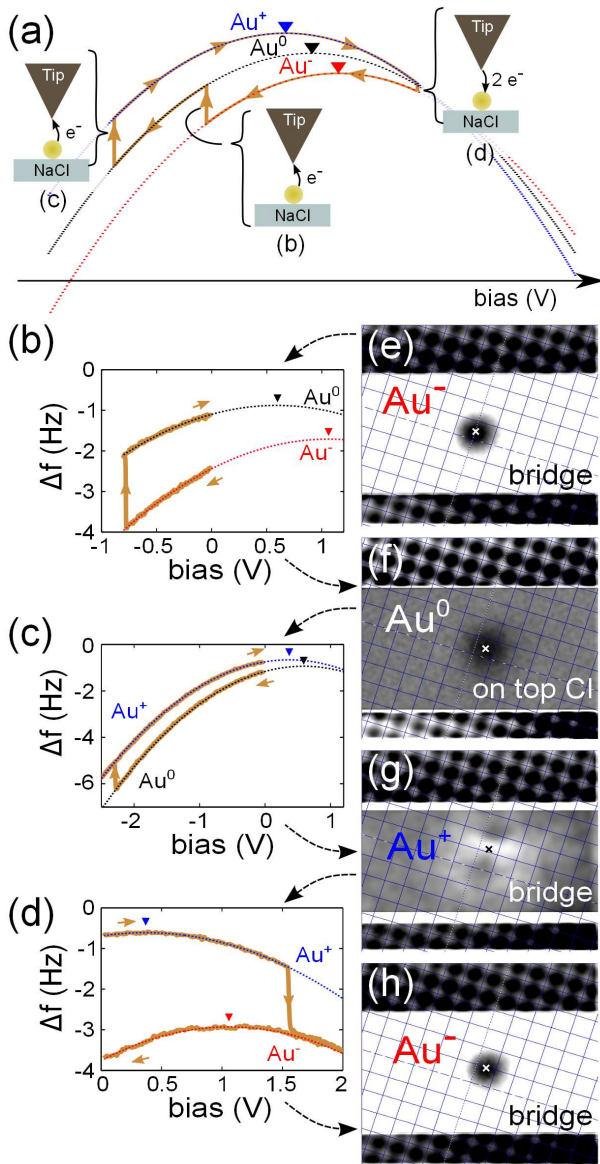


FIG. 1: Manipulation of the charge state of an Au adatom on NaCl(10 ML)/Cu(111) by attaching/detaching single electrons via a probe tip. (a) Schematic $\Delta f(V)$ spectrum of a closed charge-switching cycle ($\text{Au}^- \rightarrow \text{Au}^0 \rightarrow \text{Au}^+ \rightarrow \text{Au}^-$). The dotted parabolas visualize the change of the LCPD (triangles) by a change of the charge state. (b–d) Experimental manipulation spectra for step-wise manipulation from $\text{Au}^- \rightarrow \text{Au}^0$, $\text{Au}^0 \rightarrow \text{Au}^+$, and $\text{Au}^+ \rightarrow \text{Au}^-$, respectively. In each case, the tip was moved above the Au adatom in constant- Δf mode and then the feedback loop was interrupted. (e–h) Determination of the adsorption position at each stage by constant-height Δf images with a different height set point on the NaCl substrate (top and bottom scan lines) and on the Au adatom (middle part). A blue grid is drawn on top of the Na sublattice. Black and white crosses indicate the position of the Au adatom. Imaging conditions: $V = 0$ V, $z = 13.3/8.8$ Å (top and bottom scan lines/middle part), $z = 0$ corresponds to an STM set point ($V = 4.2$ V, $I = 40$ fA) above NaCl. All images are of size 50×40 Å².

a single Au atom adsorbed on a NaCl(10 ML)/Cu(111) film. Manipulation between three different charge states (neutral, negatively charged, and positively charged) could be achieved by single-electron transfer between the tip and the adatom; the adsorption site of each charge state could be determined from AFM imaging. The charge state of the adatom was manipulated step by step in a controlled manner by applying symmetric voltage ramps (from 0 V to a certain voltage depending on the desired manipulation and back in 30 s). The change in the charge state was revealed from the behavior of the frequency shifts $\Delta f(V)$ as a function of V , as shown both schematically [Fig. 1(a)] and for three consecutively performed charge-manipulation events in Figs. 1b–d. In all cases, a jump is observed in $\Delta f(V)$ during application of the bias ramp. The $\Delta f(V)$ fall onto two distinct parabolas, which are shifted horizontally *and* vertically with respect to each other. The horizontal shift of the parabola maximum, which is a direct measure of the change of the LCPD, indicates that charge was transferred between the Au adatom and the tip at the time when the jump in $\Delta f(V)$ occurred. The vertical shift is strongly influenced by the mesoscopic properties of the tip-sample junction (so-called averaging effects) [16] and extraction of meaningful information even from the shift direction is not trivial. Figures 1e–h show atomically resolved images of the NaCl film and were obtained by recording Δf images at constant height with different height set-points on the NaCl substrate and above the Au adatom. The Au adsorption site was obtained using the imaged sublattice of Na atoms as a reference [12].

Prior to the charge manipulation experiment, after STM imaging at large positive bias, the Au adatom was negatively charged in a site bridging two Na atoms [Fig. 1(e)]. Application of the bias ramp induced a jump to a less negative Δf at -0.8 V, see Fig. 1b. The corresponding LCPD shift to smaller bias voltage after the jump indicated that negative charge was transferred from the Au adatom to the tip. The Au adatom then ended up being neutral in a site on top of a Cl atom [Fig. 1(f)]. Application of the bias ramp, shown in Fig. 1c, shifted the LCPD further to a smaller bias voltage. The Au adatom now appeared as a faint protrusion accompanied by two shallow dimples that were separated by more than a lattice spacing [Fig. 1(g)]. This protrusion, which we identify as the position of a positively charged Au adatom [17], was slightly off-center of the bridge position. No further changes in the Δf signal were observed upon ramping the bias to -4 V. The reversal of the sign of the bias ramp [Fig. 1(d)] restored the initial charge state of the Au adatom, which was characterized by a significantly greater LCPD value and adsorption in an equivalent but different bridge position as the one in Fig. 1b. Note that the attachment/detachment of an electron to/from the Au adatom causes its adsorption position to change [see Figs. 1(e–h)] and, therefore, the

Au atom will move laterally under the tip in the course of a closed charge-switching cycle. This motion also affects the vertical and the horizontal shift of the parabolas shown in Figs. 1b–d. However, the effect on the horizontal shift is small enough so that its direction still reflects the change of the charge state (towards being more positive or negative).

Five more closed charge-switching cycles ($\text{Au}^- \rightarrow \text{Au}^0 \rightarrow \text{Au}^+ \rightarrow \text{Au}^-$) were recorded in succession without tracking the position of the Au adatom in between. The energies at which the individual electron attachment/detachment processes occurred varied statistically, but were all found within ± 0.3 V of the jump positions observed in Figs. 1b–d. Note that this allows us to set the charge state on demand. For example, Au^+ is set by ramping V to -2.5 V, Au^- by ramping V to $+2.0$ V, and Au^0 by first switching to Au^- and then ramping V to -1.0 V.

The charge state can be read out without manipulating it by determining the LCPD. Joint fitting of the corresponding $\Delta f(V)$ spectra (covering the range from -4 to $+4$ V) yields LCPD values of 770 ± 110 , 620 ± 40 , and 420 ± 20 mV for Au^- , Au^0 and Au^+ , respectively. For the fit, the same curvature was assumed for all charge states and free parameters were used to capture the horizontal and vertical shifts of the segments of the parabolas. Within the experimental uncertainty, we find that the LCPD shifts almost equidistantly by approximately 200 mV per unit charge on a NaCl(10 ML) film. The distinct LCPD values for the three charge states enable detection of the charge state of single Au adatoms even at large tip-sample distances for which the tunneling probability through the vacuum gap vanishes. Note, however, that the charge state can also be measured at short tip-sample distances without changing the charge state for $\Delta f(V)$ spectra recorded between -0.6 and $+1.3$ V [see Figs. 1(b–d)]. We believe that the fact that the Au^0 charge state is not observed on the way back from Au^+ to Au^- is related to the system's energetics and different energy barriers for electron attachment to an Au cation as compared to electron attachment to neutral Au.

Experimental control of the charge state via ramping the bias allowed us to set neighboring Au adatoms to Au^- , Au^0 , and Au^+ (see Fig. 2). Using constant Δf feedback, a topographic AFM image of the ensemble could be obtained without altering the charge state of the individual Au adatoms during image acquisition. The height profiles shown in the inset figure reveal markedly different apparent heights for the three charge states in agreement with the constant height images presented in Figs. 1e–h.

We performed similar charge-manipulation experiments as the one shown in Fig. 1 for all film thicknesses between 2 and 11 ML, as well as for NaCl films grown on the Cu(100) and Cu(311) substrates. Tristate charge control of Au adatoms was achieved for all film thicknesses and crystallographic orientations of the copper

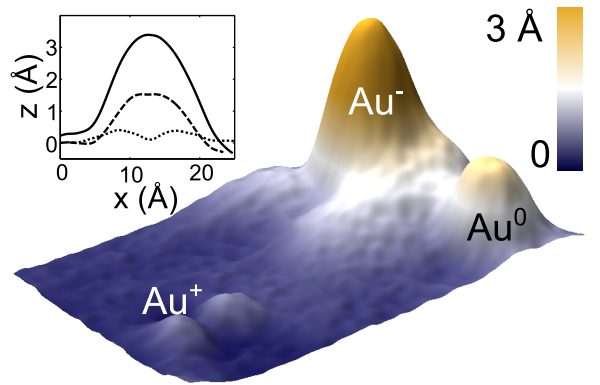


FIG. 2: Three-dimensional topographical AFM image of three Au adatoms on a NaCl(10 ML)/Cu(111) film with charge states neutral, positively charged, and negatively charged. Height profiles are shown in the inset figure (solid line: Au^- , dashed line: Au^0 , dotted line: Au^+). Imaging details: Const. Δf feedback, $\Delta f = 2$ Hz, $V = 0$ V, image size $60 \times 35 \text{ \AA}^2$.

substrate. However, as will be discussed below, the Au^0 and Au^+ states spontaneously decayed into Au^- on thin NaCl films of only few monolayers supported by Cu(311). On all Cu substrates, and irrespective of the film thickness, the neutral Au adatom was observed on top of a chlorine atom, and in the bridge position both for the negative and the positive charge state. Our results thus expand the scope of charge-state control as compared to earlier work [3], where only Au^0 and Au^- were reported to be stable and where it had only been investigated for NaCl(2, 3 ML) films. [18]. We note that the Au cation has similarities to the $(\text{AgCl}_2)^-$ -complex reported in Ref. 4.

In contrast to the Cu(100) and Cu(111) substrates, we observed that Au atoms on NaCl(2–4 ML)/Cu(311) films were negatively charged directly after Au deposition. Attempts to set the neutral and positive Au charge states via the probe tip failed on these film thicknesses. Only on film thicknesses ≥ 5 ML could we perform the kind of charge-manipulation experiment shown in Fig. 1. For 3- and 4-ML-thick NaCl films, we could measure the lifetime of the Au^0 state by applying a sample bias of $V = -1.7$ V, which allowed us to detach the electron from the Au anion as soon as it got charged via the Cu(311) substrate. The charge state of the Au adatom was detected via the Δf signal, and time lapse spectra were recorded. A typical spectrum, recorded on a NaCl(4 ML) film, is shown in Fig. 3; the white arrow in the STM image [Fig. 3(a)] indicates the position of the tip. The height of the tip above the Au atom was adjusted to keep perturbations by the electric field of the tip low while maintaining a reasonable tunneling probability across the vacuum gap. At the tip–Au distance of 8 \AA chosen, the neutral and the negative charge states are well separated in the Δf signal, and the lifetime of the Au^- charge state is on the

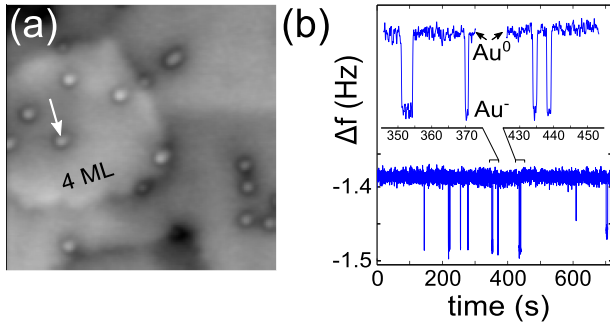


FIG. 3: Lifetime measurement of the Au^0 state on $\text{NaCl}(4 \text{ ML})/\text{Cu}(311)$. (a) STM topography image indicating the position of the tip during data acquisition; the tip was positioned 8 \AA above the Au adatom. Imaging conditions: $V = 1.5 \text{ V}$, $I = 20 \text{ fA}$, image size $200 \times 200 \text{ \AA}^2$. (b) Time lapse of the Δf signal, reflecting the charge state of the Au adatom. A bias of $V = -1.7 \text{ V}$ was applied to transfer the electron from the Au anion to the tip.

order of seconds, see Fig. 3b. The time between the Au^- spikes indicates a lifetime of the Au^0 state on the order of 50 s on the $\text{NaCl}(4 \text{ ML})$ film. On $\text{NaCl}(3 \text{ ML})$, see SM, the lifetime of the Au^0 state is at the detection limit imposed by the frequency and amplitude control loops of the AFM force sensor, which are approximately 0.5 s.

In Ref. 4, the key parameters determining the stability of various charge states are discussed within a simple model. Based on this model, we ascribe the spontaneous decay of the Au^0 and Au^+ charge states on NaCl films grown on $\text{Cu}(311)$ to the significantly reduced work function of $\text{Cu}(311)$ (4.31 eV [13], as compared to 4.59 eV for $\text{Cu}(100)$ and 4.94 eV for $\text{Cu}(100)$ [14]), which shifts the affinity level of Au^0 for an unrelaxed ion lattice closer to the Fermi level of the $\text{Cu}(311)$ substrate ($\approx 0.8 \text{ eV}$ above E_F [19]). Since this affinity level is phonon broadened, phonon-mediated charging of the Au adatom by an electron tunneling from the $\text{Cu}(311)$ substrate through the NaCl film becomes a possible process. In a simplistic model, the likelihood of this process is given by the product of two probabilities: (i) the probability that the Au^0 affinity level is temporarily pushed below the Fermi level by a phonon, and (ii) the probability for an electron to tunnel through the NaCl film. The former depends on the alignment of the Au^0 affinity level with respect to the Fermi level and its vibrational broadening; the latter probability decreases exponentially with increasing film thickness.

Large ionic relaxations within the NaCl film are responsible for the fact that the Au^- charge state is stable and cannot spontaneously decay to the neutral state on films with a high tunneling probability between substrate and adatom. These relaxations cause a realignment of the electronic levels of the Au adatom and shift the Au^0 affinity level well below the Fermi level of the metal substrate. Our work paves the way to a direct

determination of the ionic relaxation energy of charged, adsorbed single atoms, as well as the relaxation energy of single molecules, in the future. The energy at which the attachment/detachment of an electron is observed in Fig. 1 is directly related to the relaxation energy; however, it is influenced by the tip-adatom distance and by vibrational broadening of the affinity/ionization level.

In summary, we have shown charge-state manipulation of single Au atoms on $\text{NaCl}(2\text{--}11 \text{ ML})$ films by attaching/detaching single electrons via the tip of an AFM. The fact that the AFM is a very sensitive probe with single-electron sensitivity and does not rely on charge tunneling allows us to monitor the charge-manipulation process in detail, revealing the instant of the electron passage as well as its direction. Furthermore, our results provide physical insight into the transition from few ML thick films to bulk-like insulating films with vanishing tunneling probability in the context of charge-state stability. This prepares the ground for future single-electron-transport experiments where suppressing charge transfer with the substrate is highly desired because charge-state stabilization becomes independent of material properties, more charge states are accessible, and charge leakage to the substrate is also suppressed for charge transfer between adsorbates.

We thank R. Allenspach for helpful comments. Financial support by the EU projects ‘ARTIST’ (Contract No. 243421), ‘PAMS’ (Contract. No. 610446) and the ERC Advanced Grant ‘CEMAS’ is acknowledged.

* Electronic address: wst@zurich.ibm.com

- [1] M. Sterrer, T. Risse, U. Martinez Pozzoni, L. Giordano, M. Heyde, H.-P. Rust, G. Pacchioni, and H.-J. Freund, *Phys. Rev. Lett.* **98**, 096107 (2007).
- [2] M. Yulikov, M. Sterrer, M. Heyde, H.-P. Rust, T. Risse, H.-J. Freund, G. Pacchioni, and A. Scagnelli, *Phys. Rev. Lett.* **96**, 146804 (2006).
- [3] J. Repp, G. Meyer, F. E. Olsson, and M. Persson, *Science* **305**, 493 (2004).
- [4] F. E. Olsson, S. Paavilainen, M. Persson, J. Repp, and G. Meyer, *Phys. Rev. Lett.* **98**, 176803 (2007).
- [5] L. Gross, F. Mohn, P. Liljeroth, J. Repp, F. J. Giessibl, and G. Meyer, *Science* **324**, 1428 (2009).
- [6] I. Swart, T. Sonnleitner, and J. Repp, *Nano Lett.* **11**, 1580 (2011).
- [7] P. Frondelius, A. Hellman, K. Honkala, H. Häkkinen, and H. Grönbeck, *Phys. Rev. B* **78**, 085426 (2008).
- [8] J. Jung, H.-J. Shin, Y. Kim, and M. Kawai, *Phys. Rev. B* **82**, 085413 (2010).
- [9] M. Sterrer, T. Risse, M. Heyde, H.-P. Rust, and H.-J. Freund, *Phys. Rev. Lett.* **98**, 206103 (2007).
- [10] F. J. Giessibl, *Applied Physics Letters* **73**, 3956 (1998).
- [11] W. Steurer, L. Gross, and G. Meyer, *Applied Physics Letters* **104**, 231606 (2014).
- [12] G. Teobaldi, K. Lämmle, T. Trevethan, M. Watkins, A. Schwarz, R. Wiesendanger, and A. L. Shluger, *Phys.*

- Rev. Lett. **106**, 216102 (2011).
- [13] F. E. Olsson, M. Persson, J. Repp, and G. Meyer, Phys. Rev. B **71**, 075419 (2005).
- [14] P. O. Gartland, S. Berge, and B. J. Slagsvold, Phys. Rev. Lett. **28**, 738 (1972).
- [15] Supplementary materials: Sample preparation; Conduction-band STM imaging of NaCl; Charge-state stability of Au adatoms on NaCl/Cu(311) films
- [16] A manuscript addressing these issues in detail is in preparation.
- [17] As not shown here, the Au^+ adatom was found in two equivalent configurations that were rotated by 90° with respect to each other.
- [18] For Au^- , the adsorption site reported in Ref. 3 is in apparent contradiction to the one reported here. Detailed investigations revealed that adsorption on top of a chlorine atom on bilayer NaCl films is a special case of a much richer variability, the details of which will be published elsewhere.
- [19] Estimated from the Au^0 affinity level on NaCl(2 ML)/Cu(111) (see Ref. 3) and the work function difference between the Cu(311) and Cu(111) substrates.